remote sensing

Article

# Dynamic Simulation and Prediction of Carbon Storage Based on Land Use/Land Cover Change from 2000 to 2040: A Case Study of the Nanchang Urban Agglomeration

**Yuheng Fu [1], Min Huang [1,2,3,4,*], Daohong Gong [1,2], Hui Lin [1,2], Yewen Fan [3] and Wenying Du [4]**

1 School of Geography and Environment (School of BeiDou Industry)/Key Laboratory of Poyang Lake Wetland and Watershed Research (Ministry of Education), Jiangxi Normal University, Nanchang 330022, China; fuyuheng@jxnu.edu.cn (Y.F.); gongdaohong@jxnu.edu.cn (D.G.); huilin@cuhk.edu.hk (H.L.)
2 Nanchang Base of International Centre on Space Technologies for Natural and Cultural Heritage under the Auspices of UNESCO, Jiangxi Normal University, Nanchang 330022, China
3 State Key Laboratory of Information Engineering in Surveying, Mapping and Remote Sensing, Wuhan University, Wuhan 430079, China; fyw@whu.edu
4 National Engineering Research Center for Geographic Information System, China University of Geosciences, Wuhan 430074, China; duwenying@cug.edu.cn
* Correspondence: huangm@jxnu.edu.cn



**Citation:** Fu, Y.; Huang, M.; Gong, D.; Lin, H.; Fan, Y.; Du, W. Dynamic Simulation and Prediction of Carbon Storage Based on Land Use/Land Cover Change from 2000 to 2040: A Case Study of the Nanchang Urban Agglomeration. *Remote Sens.* **2023**, *15*, 4645. https://doi.org/10.3390/rs15194645

Academic Editors: Guoqing Zhou, Yuefeng Wang and Oktay Baysal

Received: 30 August 2023
Revised: 12 September 2023
Accepted: 18 September 2023
Published: 22 September 2023



**Abstract:** Land use/land cover change (LUCC) constitutes a significant contributor to variations in the storage of carbon within ecosystems and holds substantial significance within the context of the carbon cycling process. This study analyzed land use data from the Nanchang urban agglomeration in 2000 and 2020 to investigate changes in land use and carbon storage using the PLUS model and GIS. The results show the following: (1) From 2000 to 2020, the Nanchang urban agglomeration experienced reductions in the extents of croplands, woodlands, grasslands, and unused lands. The predominant trend in land transformation involved the conversion of cropland into built-up land. (2) Between 2000 and 2020, there was a declining trajectory observed in carbon storage for the Nanchang urban agglomeration, with an overall decrease of $1.13 \times 10^7$ t. The space is characterized by a high-altitude perimeter and a low-altitude center. Urbanization's encroachment on cropland is the main reason for declining carbon storage. (3) The predictive outcomes reveal that, in 2040, carbon storage in the Nanchang urban agglomeration will be reduced by $1.00 \times 10^7$ t under the natural development scenario, and reduced by $3.90 \times 10^6$ t and increased by $2.29 \times 10^5$ t, respectively, under the cropland protection and ecological protection scenarios. The risk of carbon loss is significantly reduced by ecological protection policy interventions. Our analysis of the land use patterns and carbon storage distribution in the Nanchang urban agglomeration over the past 20 years and our exploration of the land use change trend over the next 20 years under the conservation policy provide a reference basis for increasing the carbon sink in the core area of the ecological city cluster of Poyang Lake and realizing the sustainable development of the city.

**Keywords:** carbon storage; InVEST model; land use/land cover change; Nanchang urban agglomeration; PLUS model

## 1. Introduction

Global climate change is a major obstacle to human development, with anthropogenic carbon emissions being one of the main drivers of climate change [1–3] and land use/land cover change being the second-largest source of emissions [4,5]. This change affects the way materials and energy move along terrestrial ecosystems and alters carbon sources and sinks [6–8]. To combat global warming, China has committed to reaching a carbon peak by 2030 and advancing towards carbon neutrality by 2060 [9,10]. The government has implemented a series of significant initiatives aimed at improving peoples' livelihoods, including afforestation and grassland restoration, which have greatly modified the association between land utilization and the capacity for carbon storage, as well as affecting soil carbon sequestration [11]. Soil carbon storage is a crucial factor when evaluating the sustainable growth of land-based ecosystems [12]. Studying how to achieve carbon emissions reduction and carbon sequestration through land use adjustments is currently a research hotspot [13,14]. Against the backdrop of urbanization in China, urban agglomerations have become significant drivers of regional economic development [15]. Investigating the correlation and impacts between carbon storage and land use change is essential for the country's green and sustainable development [16,17]. The Jiangxi provincial government has issued the document "Development Plan of Nanchang Urban Agglomeration (2019–2025)", which provides guidance for low-carbon urban development and territorial spatial planning during this important time of pursuing the dual carbon policies. This serves as a valuable reference for achieving the dual carbon goals. The Nanchang urban agglomeration, known for its prominent ecological features, is a key area for high-quality, leapfrog development in Jiangxi Province. It holds the status of an exemplar area for green and sustainable development within the Yangtze River Economic Belt. As a pivotal region for economic advancement within Jiangxi Province, it progressively assumes a pivotal role as a significant spatial entity.

With carbon storage becoming a research hotspot, more scholars are investigating and exploring estimation methods for carbon storage, covering various aspects. Early methods mainly included field sampling, the calculation method [18], the remote sensing estimation method [19,20], and the model estimation method [21]. These methodologies have been applied in various research areas, including different land use types [22], large-scale provincial and municipal levels [23], watersheds [24], and representative ecological regions [25]. Comprehensive studies conducted by Leh et al. [26], He et al. [27], Babbar et al. [28], and Wang et al. [29] indicate that the InVEST model is a widely used method. Compared with other models, this model requires less imported data and outputs more data, has multiple modules, adopts multilevel design, and can be analyzed at multiple scales and in multiple contexts. Particularly, it is suitable for large-scale carbon storage assessment and advantageous in rapidly calculating regional carbon storage. Subsequently, researchers began to concentrate on estimating future carbon storage, and researchers usually used land use simulation coupled with carbon storage estimation models. Commonly used models include CA-Markov [30], FLUS [31,32], Clue-s [33], and PLUS [34]. Studies have found that among these models, the PLUS model performs well in simulating fragmented patches, especially for research areas with many small patches [35]. Meanwhile, although investigations have been conducted on the integration of future land use simulation models with the InVEST model, previous research has mainly focused on the "constraint" effect of policies on future land use patterns, lacking attention to the "driving" and "guiding" effects of policies on LUCC [22,36,37]. Within the existing literature, research on carbon storage estimation in China has mainly focused on fields such as forest vegetation carbon storage [38,39], soil organic carbon storage [40], ecosystem carbon storage [41], and carbon trading [42], with less coverage of other scopes. Against the backdrop of urbanization in China, urban agglomerations have become important engines for regional economic development, and extensive domestic and international research has already established the noteworthy influence of urban expansion on the ecosystem carbon storage balance [27,43,44]. The application of novel models such as the PLUS model to simulate future land use changes, especially throughout the entire Nanchang urban agglomeration, remains relatively uncommon in the current literature.

Based on the above background, this study took the Nanchang urban agglomeration as its research object, coupling the widely used and effective InVEST and PLUS models to analyze future trends of land use spatial patterns and carbon storage. Relying on land use data from 2000 and 2020, the carbon storage module of the InVEST model was employed to assess alterations in ecosystem carbon storage within the region spanning a 20-year timeframe. Additionally, this study conducted simulations to evaluate carbon storage across diverse land use categories in the Nanchang urban agglomeration by the year 2040. Poyang Lake is an important ecological barrier in the middle reaches of the Yangtze River Economic Belt, and predicting the relationship between land and carbon storage in the urban agglomeration where it is located is a matter of ecological security.

## 2. Materials and Methods

### *2.1. Study Area*

The Nanchang urban agglomeration is located in the northern region of Jiangxi Province, bordered to the north by the Yangtze River, encompassing significant natural advantages with the presence of Lushan Mountain and Poyang Lake. As shown in Figure 1, the Nanchang urban agglomeration, with an elevation ranging from 0 to 1960 m, experiences a subtropical monsoon climate. The western region is primarily composed of mountainous hills, while the eastern region consists of plains along the lakeshore. The topography exhibits a gradual elevation increase from east to west in the region. The regional forest resources are abundant, with the predominant forest type being evergreen broadleaf forests. The average yearly temperature fluctuates between 9 and 19 degrees Celsius, while the mean annual precipitation varies from 1900 to 2500 mm. The agglomeration covers 25 counties and cities, including Nanchang, Jiujiang, Yichun, Shangrao, Fuzhou, and the Ganjiang New District. It covers an area of around $4.5 \times 10^4$ square kilometers, accounting for 26.96% of Jiangxi Province. By the conclusion of 2020, the cumulative population had reached 17.41 million people, accounting for 38.53% of the province's population. The regional gross domestic product (GDP) amounted to 178.3 billion dollars, representing 49.98% of the province's total. The Nanchang urban agglomeration is a critical part of the Yangtze River Economic Belt. In this region, Poyang Lake, as the largest freshwater lake in China, plays a crucial role in supporting multiple ecological functions, such as regulating runoff, purifying water bodies, and controlling the climate. It hosts a diverse range of biological resources, including a large population of fish and various bird species. The study of carbon storage in the Nanchang urban agglomeration holds profound importance for the ecological development of the central region in China.

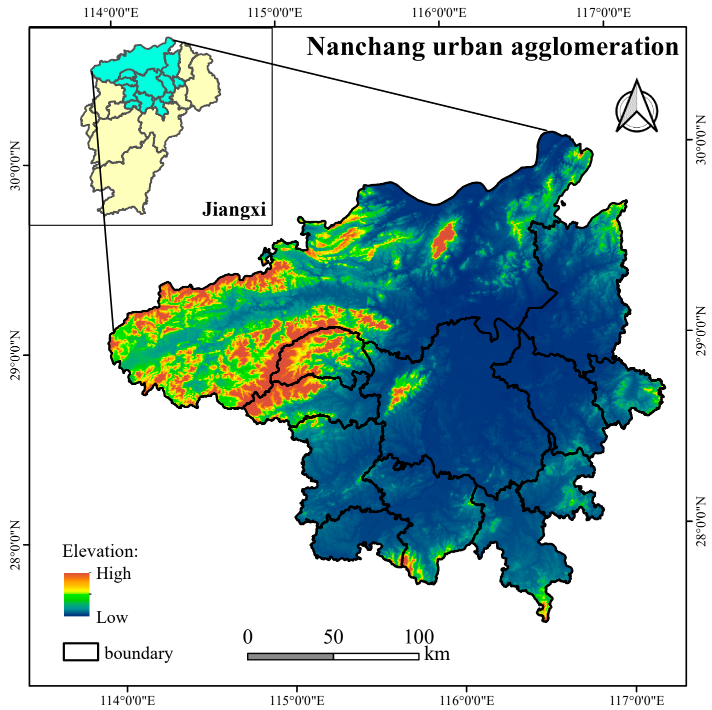


**Figure 1.** Overview of the Nanchang urban agglomeration.

### *2.2. Data Sources*

The research dataset in this study encompasses land use data, socioeconomic data, and natural condition data, obtained from various sources listed in Table 1. Specifically, the land use/land cover change (LUCC) data for the years 2000 and 2020 are derived from the GLOBELAND30 dataset (30 m spatial resolution) generated by the National Geomatics Center of China (http://www.globallandcover.com, accessed on 14 April 2023). The land use types within the research area were redefined into six distinct classifications: cropland, woodland, grassland, water body, built-up land, and unused land. Gross domestic product (GDP), population density, average annual temperature, annual precipitation, and soil type data (all with a spatial resolution of 1 km) were obtained from the Data Center for Resources and Environmental Sciences of the Chinese Academy of Sciences (https://www.resdc.cn, accessed on 14 April 2022). Digital elevation model (DEM) data (30 m spatial resolution) were obtained from the ASTER GDEM dataset, which were available on the Geographic Spatial Data Cloud (http://www.gscloud.cn, accessed on 14 April 2022). The transportation road network data were obtained from OpenStreetMap (www.openstreetmap.org, accessed on 14 April 2022). All the aforementioned data were subjected to resampling, resulting in a grid resolution of 30 m by 30 m, accomplished through the utilization of ArcMap.

**Table 1.** Details of LUCC and driving factors data.

| Category | Data | Data Resource | Original Resolution (m) |
|---|---|---|---|
| Land use data | Land use in 2000 and 2020 | GlOBELAND30 dataset (http://www.globallandcover.com/, accessed on 14 April 2022) | 30 |
| Natural factors | DEM<br>Slope | Geospatial Data Cloud (http://www.gscloud.cn/, accessed on 14 April 2022) | 90<br>90 |
| | Temperature<br>Precipitation<br>Soil type | Data Center for Resources and Environmental Sciences ofthe Chinese Academy of Sciences (https://www.resdc.cn, accessed on 14 April 2022) | 30<br>30<br>30 |
| Socioeconomic factors | Population<br>GDP | Data Center for Resources and Environmental Sciences ofthe Chinese Academy of Sciences (https://www.resdc.cn, accessed on 14 April 2022) | 30<br>30 |
| | Distance to primary roads<br>Distance to secondary roads<br>Distance to tertiary roads | OpenStreetMap (https://www.openstreetmap.org/, accessed on 14 April 2022) | 1000<br>1000<br>1000 |
| | Distance to rivers | National Catalogue Service for Geographic Information (https://www.webmap.cn/, accessed on 14 April 2022) | 1000 |

### *2.3. Research Methods*

The study structure comprised two sections: (1) simulating LUCC data using the PLUS model and (2) evaluating ecosystem carbon storage changes attributed to LUCC with the InVEST model, as illustrated in Figure 2. Specifically, this study employed a coupled approach involving the PLUS and InVEST models to comprehensively investigate the LUCC dynamics within the Nanchang urban agglomeration. Historical land use data from 2000 and 2020 were utilized as the foundation for the simulation of LUCC scenarios for the year 2040, encompassing the policy-driven trajectories of three diverse scenarios. Through the application of the InVEST model, an in-depth analysis of carbon storage was conducted to reveal the potential impact of the current land use patterns on the carbon storage capacity within the Nanchang urban agglomeration.

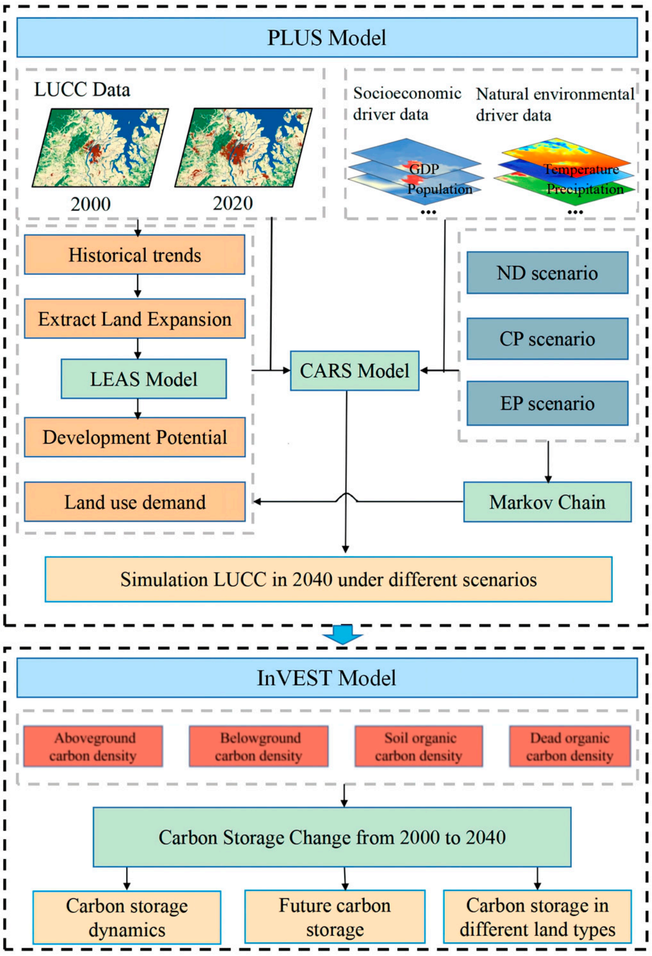


**Figure 2.** Research framework.

### 2.3.1. Assessment of Carbon Storage Based on the InVEST Model

Carbon storage is a vital regulatory ecosystem service, whereby carbon elements are immobilized within soil and vegetation to regulate atmospheric carbon levels, thereby playing a pivotal role in mitigating climate change. The InVEST model currently stands as one of the most extensively utilized models for the estimation of carbon storage in large-scale ecosystem assessments. Within the carbon storage module of the InVEST model, ecosystem carbon storage is categorized into four fundamental reservoirs: aboveground biomass carbon (carbon contained in all living plants above the soil), belowground biomass carbon (carbon present in the active root systems of plants), soil carbon (carbon distributed within organic and mineral soils), and dead organic carbon (carbon found in litter, fallen or standing dead wood). The calculation formulas for these reservoirs are as follows:

$$C_i = C_{above} + C_{below} + C_{soil} + C_{dead} \tag{1}$$

$$C_{total} = \sum_{i=1}^{n} C_i \times A_i\,,\ (i = 1, 2, \ldots, n) \tag{2}$$

where $C_i$ represents the carbon density on land use type i (t/ha); $C_{above}$ represents the carbon density of aboveground biomass (t/ha); $C_{below}$ represents the carbon density of belowground biomass (t/ha); $C_{soil}$ represents the carbon density of soil (t/ha); $C_{dead}$ represents the carbon density of dead matter (t/ha); $C_{total}$ represents the total ecosystem carbon storage (t); $A_i$ represents the total area of land use type i ($hm^2$); and n is the total number of land use types.

The carbon storage module within the InVEST model operates based on the foundational assumption that the carbon density of each land cover type remains invariant. Subsequently, the calculation of regional vegetation carbon storage is derived by the multiplication of the unchanging carbon density values associated with various vegetation types by their respective spatial extents. Since different researchers have obtained significant variations in carbon density, it is preferable to select literature data that focus on the southern region, particularly the Poyang Lake Basin, as references. For LULC types with insufficient data, we consulted information from the China Terrestrial Ecosystem Carbon Density Dataset and comparable regions to ultimately enhance the required carbon density data [45,46] (Table 2).

**Table 2.** Carbon intensity of each land use type in the area (t/hm$^2$).

| Land Use Type | Aboveground Carbon Density | Belowground Carbon Density | Soil Organic Carbon Density | Dead Organic Matter Carbon Density | Total Carbon Density |
|---|---|---|---|---|---|
| Cropland | 3.55 | 2.09 | 32.34 | 0.54 | 38.52 |
| Woodland | 46.9 | 11.2 | 42.3 | 0.69 | 101.09 |
| Grassland | 1.02 | 8.45 | 52.52 | 0.43 | 62.42 |
| Water body | 0.08 | 0.07 | 0.00 | 0.00 | 0.15 |
| Built-up land | 1.49 | 0.35 | 0.04 | 0.00 | 1.88 |
| Unused land | 0.36 | 0.53 | 1.81 | 0.03 | 2.73 |

### 2.3.2. Prediction of Future LUCC Based on the PLUS Model

The PLUS model is a patch-level land use change simulation model developed by the High-Performance Spatial Computing Intelligence Laboratory situated at China University of Geo-sciences (Wuhan). It is based on raster data and utilizes the Land Expansion Analysis Strategy (LEAS) integrated with the Clustered Autonomous Random Seeds (CARS) framework. Technical terms are explained upon first use. The model has the ability to comprehensively capture the influences of diverse driving factors on land use change dynamics and to simulate various land use categories across distinct scenarios using either Markov chains or linear regression methods.

Utilizing land use data from the years 2000 and 2020 as its foundational dataset, this study applied a 20-year time interval to simulate the prospective land use conditions within the Nanchang urban agglomeration for the year 2040. Through the utilization of the Land Expansion Analysis Strategy (LEAS) module within the PLUS model, we obtained the probabilities associated with the evolution of various land use types within the Nanchang urban agglomeration, spanning the period from 2000 to 2020. We subsequently applied the Markov chain methodology to compute the projected land use requirements for the year 2040. Following this, we harnessed the Clustered Autonomous Random Seeds (CARS) module, in conjunction with the 2020 land use data and the previously derived development probabilities, to generate various scenarios for the year 2040. To enhance the fidelity of these predictions, we adjusted the transfer cost matrix based on the observed changes in land use types within the Nanchang urban agglomeration from 2000 to 2020. Moreover, we determined neighborhood weights, which served as indicators of the expansion intensity of distinct land use categories. These neighborhood weights fall within a threshold range of 0 to 1, with values closer to 1 signifying greater expansion potential. Additionally, we established the scenarios of natural development, cropland protection, and ecological conservation.

Based on the 2000 land use data, 11 driving factors were inputted into the land use demand for the year 2000. Transition matrices were established using Markov transition probabilities from 2000 to 2020. Neighborhood weights were assigned based on the proportion of land type changes. The land use demand for the year 2020 was simulated, and the simulated land use status was compared to the actual 2020 land use to assess model simulation accuracy. The overall accuracy, as measured by the Kappa coefficient, was

83.16%, with a Kappa coefficient of 0.78, indicating a high level of confidence in the results generated by the PLUS model.

(1) Natural development scenario (ND scenario): This scenario entails preserving the existing pattern of land use structural changes and keeping the transfer probabilities unchanged. Since there is minimal mutual transfer between unused land and other land use types within the Nanchang urban agglomeration under this scenario, the transfer cost matrix was set as 0 for unused land and 1 for the rest. In accordance with the historical trajectory of land use evolution from 2000 to 2020 and the insights gained from Markov chain analysis, the land use requirements for 2040 were established, reflecting the historical development trend.

(2) Cropland protection scenario (CP scenario): This scenario also entails the preservation of the established pattern of structural changes in land use and the maintenance of unaltered transfer probabilities. Similar to the natural development scenario, the transfer cost matrix was configured with a value of 0 for unused land and a value of 1 for the remaining land use types. Building upon the natural development scenario, in alignment with the "National Land Use Master Plan Outline" (2006–2020), the Development Plan for the Nanchang urban agglomeration (2019–2025), and the Spatial Master Plan for Nanchang City (2021–2035), cropland protection measures are implemented to strictly control the total amount of cropland and promote intensive land use. Then, with reference to previous studies, by modifying the 2000–2020 Markov transformation probability matrix, the transfer probability from cropland to built-up area is decreased by 30% and directed towards cropland expansion.

(3) Ecological conservation scenario (EP scenario): This scenario takes into account the efforts of the Nanchang urban agglomeration to become a strategic hub for the green ecological corridor. The primary objective of this scenario is to impose stringent protection measures on crucial ecological areas in the metropolitan area, curb carbon storage degradation, increase woodland and grassland areas, and restrict the rapid expansion of built-up land. Building upon the cropland protection scenario, with reference to the Development Plan for the Nanchang urban agglomeration (2019–2025) and the Spatial Master Plan for Nanchang City (2021–2035), the conversion of ecologically functional cropland, grassland, and woodland to built-up areas is strictly controlled. Then, with reference to previous studies, and by modifying the 2000–2020 Markov transformation probability matrix, within the context of ecological conservation scenario, there is a 30% reduction in the likelihood of cropland conversion, accompanied by an augmentation in the likelihood of cropland transition into woodland. The probabilities of grassland and woodland conversion to cropland are reduced by 40%, with corresponding increases in grassland and woodland preservation.

The dataset for land utilization was preprocessed to serve as the input for the PLUS model. To determine the parameters for different scenarios, multiple scenarios with quantity constraints were established and combined with the Markov chain method to calculate changes in different land types. Spatial and quantitative constraints were combined to approach the multi-scenario setting of the aforementioned datasets. Tables 3 and 4 present the neighborhood weights, calculated utilizing the ratio of land use type expansion to total land expansion and the transition matrix, correspondingly.

**Table 3.** Neighborhood factor parameters.

| Land Use Type | Cropland | Woodland | Grassland | Water Body | Built-Up Land | Unused Land |
|---|---|---|---|---|---|---|
| Natural development neighborhood factor | 0.07 | 0.11 | 0.01 | 0.29 | 1.00 | 0.09 |
| Cropland protection neighborhood factor | 0.28 | 0.13 | 0.03 | 0.30 | 0.86 | 0.09 |
| Ecological protection neighborhood factor | 0.07 | 0.31 | 0.10 | 0.34 | 0.95 | 0.09 |

**Table 4.** Multiple scenario transfer matrix setting.

| | ND | | | | | | CP | | | | | | EP | | | | | |
|---|---|---|---|---|---|---|---|---|---|---|---|---|---|---|---|---|---|---|
| | a | b | c | d | e | f | a | b | c | d | e | f | a | b | c | d | e | f |
| a | 1 | 1 | 1 | 1 | 1 | 1 | 1 | 0 | 0 | 0 | 0 | 0 | 1 | 1 | 1 | 1 | 1 | 1 |
| b | 1 | 1 | 1 | 1 | 1 | 1 | 1 | 1 | 1 | 0 | 1 | 1 | 0 | 1 | 0 | 0 | 0 | 0 |
| c | 1 | 1 | 1 | 1 | 1 | 1 | 1 | 1 | 1 | 1 | 1 | 1 | 0 | 1 | 1 | 1 | 0 | 0 |
| d | 1 | 1 | 1 | 1 | 1 | 1 | 1 | 0 | 1 | 1 | 1 | 1 | 0 | 0 | 0 | 1 | 0 | 0 |
| e | 0 | 0 | 0 | 0 | 1 | 0 | 0 | 0 | 0 | 0 | 1 | 0 | 0 | 0 | 0 | 0 | 1 | 0 |
| f | 1 | 1 | 1 | 1 | 1 | 1 | 1 | 1 | 1 | 1 | 1 | 1 | 1 | 1 | 1 | 1 | 1 | 1 |

a–f indicate cropland, woodland, grassland, water body, built-up land, and unused land, respectively. A 1 means that the ground class can convert, and 0 means that the ground class cannot convert.

## 3. Results

### *3.1. LUCC Dynamics from 2000 to 2020 in the Nanchang Urban Agglomeration*

Utilizing land use transfer measurements, the Sankey diagram (depicted in Figure 3) illuminates the features of the land use configuration within the Nanchang urban agglomeration during the two decades, illustrating the transition connections between distinct land use categories. In the year 2000, the land use categories in the Nanchang urban agglomeration, ranked by area from largest to smallest, were cropland, woodland, water body, grassland, built-up land, and unused land. By 2020, the most extensive land area within the Nanchang urban agglomeration had undergone a transformation from cropland to woodland, remaining as main land classes. From 2000 to 2020, cropland, woodland, and grassland in the Nanchang urban agglomeration decreased by 1196.30 km$^2$, 445.41 km$^2$, and 383.82 km$^2$, respectively. The proportion of cropland decreased from 40.16% to 37.62%, the percentage of woodland experienced a decline from 39.52% to 38.58%, while the proportion of grassland decreased from 6.58% to 5.77%. Water bodies expanded by 673.39 km$^2$, and there was a notable increase of 1452.75 km$^2$ in built-up land, with their proportions rising by 1.43% and 3.08%. Among all land use types, cropland saw the greatest decline in proportion, while built-up land exhibited the highest growth rate. Based on the land use type transition matrix as presented in Table 5, it can be observed that from 2000 to 2020, cropland served as a significant source for the rapid expansion of built-up land in the Nanchang urban agglomeration, with 2866.91 km$^2$ transitioning out of cropland. Woodland mainly transitioned to built-up land and cropland, with 190.86 km$^2$ and 909.39 km$^2$ being converted, respectively. Although built-up land showed a clear expansion trend, 101.11 km$^2$ of it converted back to cropland, possibly due to reclamation efforts on abandoned residential land in various regions. During the period from 2000 to 2020, cropland remained the main source of conversion into built-up land, accounting for an area of 1144.68 km$^2$, while 842.38 km$^2$ and 346.53 km$^2$ of cropland converted to woodland and water body, respectively. Woodland continued to transition to built-up land and cropland, with 190.86 km$^2$ and 909.39 km$^2$ being converted, respectively.

**Table 5.** Proportion of transfers between LUCC types, 2000–2020.

| Area | Cropland | Woodland | Grassland | Water Body | Built-Up Land | Unused Land |
|---|---|---|---|---|---|---|
| Cropland | 84.85% | 4.45% | 1.83% | 2.80% | 6.05% | 0.02% |
| Woodland | 4.88% | 88.85% | 3.87% | 1.37% | 1.02% | 0.00% |
| Grassland | 12.40% | 23.67% | 51.62% | 6.25% | 5.99% | 0.07% |
| Water body | 4.90% | 0.89% | 0.60% | 92.33% | 1.03% | 0.24% |
| Built-up land | 9.84% | 0.81% | 0.52% | 1.17% | 87.65% | 0.01% |
| Unused land | 10.19% | 0.29% | 7.52% | 53.10% | 2.28% | 26.63% |

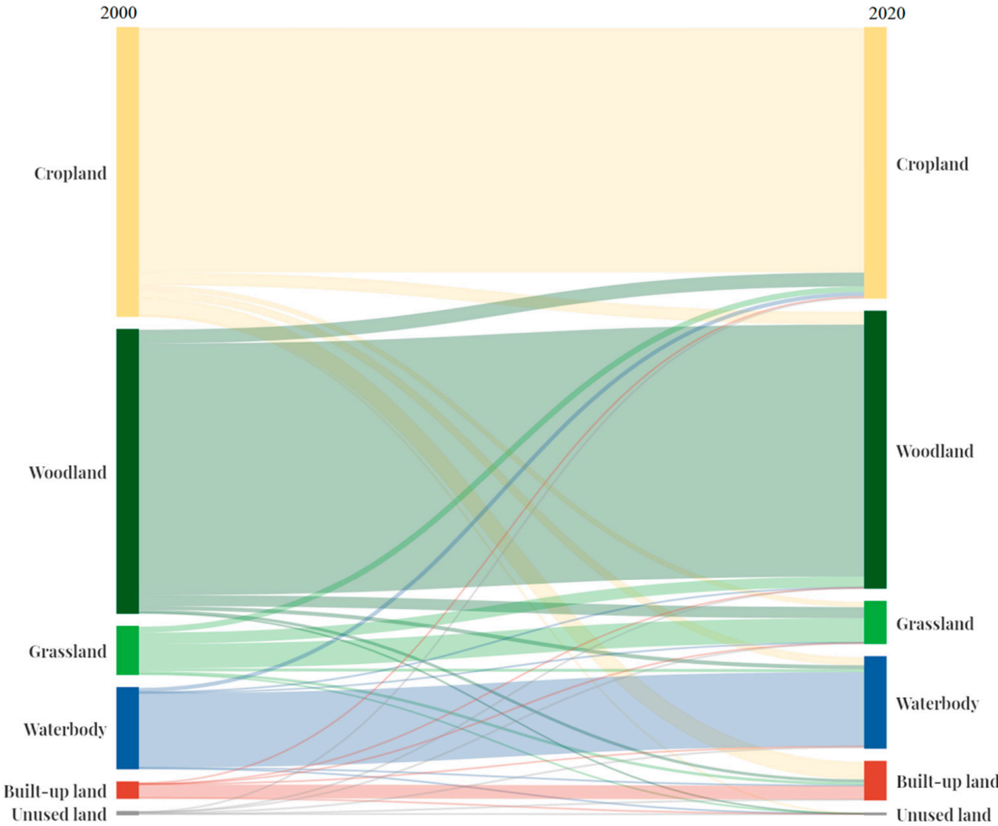


**Figure 3.** Sankey diagram of metrics for land use transfer from 2000 to 2020.

### 3.2. Analysis of LUCC Prediction Results in 2040

The simulated land use types within the Nanchang urban agglomeration for the three scenarios in 2040 are depicted in Figure 4. Upon analysis of the predicted outcomes, it became evident that when compared to the land utilization data from the year 2020, in the ND scenario, there will be a continuous increase in built-up and water body areas, with growth rates of 47.31% and 8.76%, respectively. Cropland will decrease by 5.18%, woodland area will decrease by 2.87%, and grassland area will decrease by 8.58%. Additionally, the area of unused land will decrease by 33.57%, as evidenced in Table 6. Aligned with the direction of land use conversion, it can be observed that grassland will mainly convert to cropland and woodland, with conversion areas of 333.88 km$^2$ and 98.59 km$^2$, respectively. Cropland will convert to woodland, built-up areas, and water bodies, with conversion areas of 430.19 km$^2$, 419.639 km$^2$, and 355.12 km$^2$, respectively. Water bodies will experience conversion from cropland, woodland, and grassland, while substantial land use modifications are expected for built-up land, notably from woodland and cropland.

**Table 6.** Area of each land use type under different development scenarios in 2040 and change from 2020 in the study area.

| Type | Year | Development Scenario | Cropland | Woodland | Grassland | Water Body | Built-Up Land | Unused Land |
|---|---|---|---|---|---|---|---|---|
| Area (km$^2$) | 2020 | - | 17,728.72 | 18,179.20 | 2718.48 | 5953.32 | 2480.28 | 62.73 |
| | 2040 | ND | 16,810.08 | 17,657.31 | 2485.21 | 6474.73 | 3653.73 | 41.67 |
| | | CP | 18,458.95 | 17,657.32 | 2485.22 | 5836.07 | 2648.12 | 37.05 |
| | | EP | 16,810.08 | 18,650.00 | 2550.38 | 6279.42 | 2795.79 | 37.05 |
| Annual Rate of Change (%) | 2040 | ND | −5.18% | −2.87% | −8.58% | 8.76% | 47.31% | −33.57% |
| | | CP | 4.12% | −2.87% | −8.58% | −1.97% | 6.77% | −40.94% |
| | | EP | −5.18% | 2.59% | −6.18% | 5.48% | 12.72% | −40.94% |

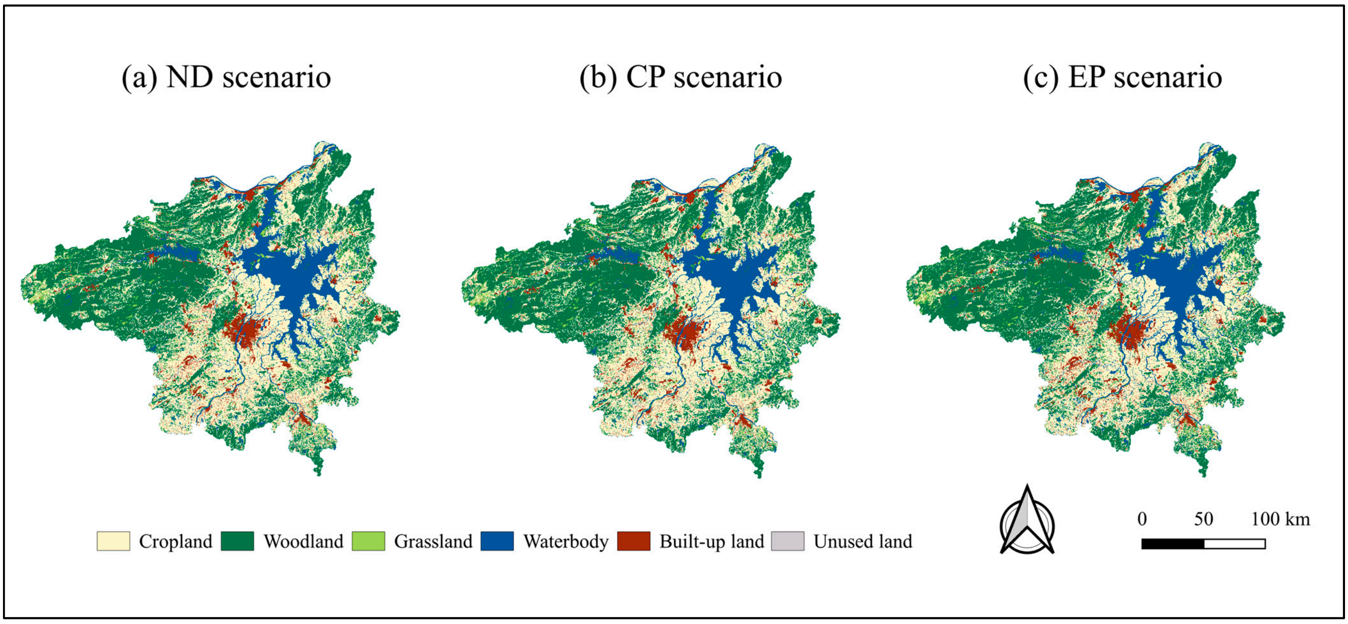


**Figure 4.** Simulation results of LUCC in 2040 under three scenarios.

In the CP scenario in 2040, a significant increase in cropland is expected in the Nanchang urban agglomeration compared to the year 2020. In the CP scenario, the projected growth rate of cropland is expected to exceed that of the ND scenario by 9.30%. However, there will be reductions in woodland, grassland, water body, built-up areas, and unused land, with woodland experiencing the largest reduction of 521.88 km$^2$. Analyzing the trajectory of land use conversion, it becomes evident that that woodland, grassland, water body, and unused land will convert to cropland. Notably, the woodland-to-cropland conversion will be the largest, totaling 540.09 km$^2$. The primary conversions for grassland will involve transitions to woodland and cropland, covering areas of 218.15 km$^2$ and 79.14 km$^2$, respectively. On the other hand, woodland will predominantly shift to cropland, grassland, and built-up areas, encompassing areas of 540.09 km$^2$, 123.11 km$^2$, and 76.99 km$^2$, respectively. Water bodies will primarily convert to cropland, with a conversion area of 108.39 km$^2$. The scenario of protected cropland under policy constraints, such as when implementing the Prevent the 'Non-grain production' of Arable Land and Stabilize Food Production Action Plan, will lead to a swift increase in cropland, accompanied by substantial reductions in the extent of grassland, woodland, water body, built-up areas, and various other land use types. In the EP scenario in 2040, a substantial augmentation of woodland is anticipated within the Nanchang urban agglomeration, with a growth rate 5.46% higher than that of the ND scenario. Woodland, grassland, built-up areas, and unused land will decrease by 2.87%, 8.58%, and 1.97%, respectively. On the other hand, cropland and built-up areas will increase by 4.12% and 6.77%, respectively. Under the ecological protection policy, the ecological land area is expected to experience a relative expansion, resulting in larger quantities of cropland, woodland, and grassland compared to the natural development scenario. Specific measures for protection will be implemented for cropland in the vicinity of Poyang Lake and the urban area of Nanchang.

### *3.3. Carbon Storage Dynamics from 2000 to 2020 in the Nanchang Urban Agglomeration*

According to calculations using the Carbon module of the InVEST model, carbon storage in the Nanchang urban agglomeration was $2.81 \times 10^8$ t in 2000 and $2.70 \times 10^8$ t in 2020. Between 2000 and 2020, there was a discernible declining trend in carbon storage within the urban agglomeration, resulting in an overall decrease of $1.13 \times 10^7$ t. In relation to land use types, the ranking of carbon storage, from highest to lowest, is as follows: woodlands, croplands, grasslands, built-up land, water body, and unused land. As urban areas expand, cropland may become fragmented into smaller parcels. Smaller cropland areas are less efficient at sequestering carbon, as they often have higher edge-to-area ratios, which can result in increased soil disturbance and reduced carbon storage. The Nanchang urban agglomeration exhibits characteristics of a developed economy, with high urbanization levels, a dense population, and extensive land development and utilization. The notable expansion of cities has led to the occupation of significant portions of cropland and woodland, thereby constituting the primary driver of the decline in carbon storage within the Nanchang urban agglomeration. The construction of roads, buildings, and other infrastructure associated with urbanization can lead to soil compaction and disruption, reducing the capacity of cropland to store carbon.

According to Figure 5, there is no substantial disparity in the spatial distribution of carbon storage within the Nanchang urban agglomeration from 2000 to 2020. Regions characterized by lower carbon storage predominantly encompass water bodies and built-up areas, whereas those with higher carbon storage are primarily composed of woodlands and grasslands. The majority of areas within the urban agglomeration exhibit minimal fluctuations in carbon storage. Reductions in carbon storage are primarily concentrated in regions where built-up land has expanded, whereas increases in carbon storage are scattered throughout newly added woodland and cropland areas. From 2000 to 2020, most areas maintained relatively stable carbon storage, while the conversion of croplands near urban areas contributed to the decline of carbon storage. Carbon storage within Lushan National Nature Reserve remained stable due to ecological protection measures like the "returning farmland to woodlands" project, showing the effectiveness of such policies in preserving carbon storage. In terms of the expansion center of the urban agglomeration, the regions exhibiting substantial variations in carbon storage are primarily concentrated in Nanchang City, notably within the Xinjian District, Honggutan District, and Anyi County. These areas are located outside the old city area of Nanchang and are new economic development zones, showing a consistent land use pattern of carbon storage reduction with the rapid expansion of urban area.

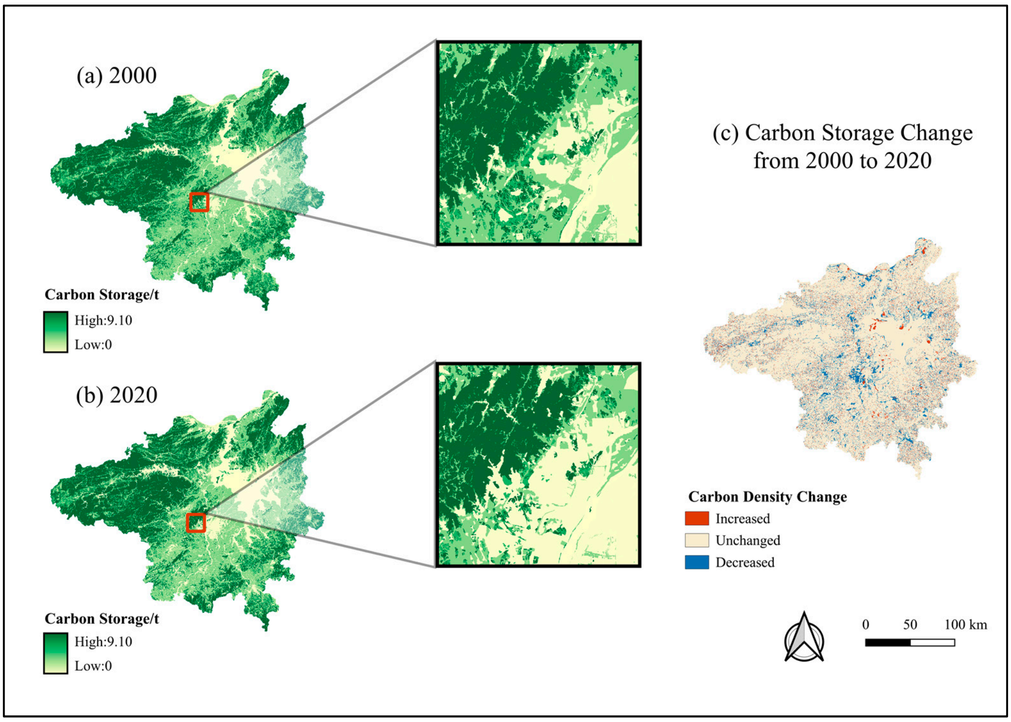


**Figure 5.** (**a**) Spatial distribution of carbon storage in 2000; (**b**) spatial distribution of carbon storage in 2020; (**c**) carbon storage change map of the study area terrestrial ecosystem from 2000 to 2020.

### 3.4. Prediction of Carbon Storage in Nanchang Urban Agglomeration in 2040

The trend analysis of carbon storage in the Nanchang urban agglomeration indicated a declining pattern from 2000 to 2020. Based on this trend, three land use scenarios for the year 2040 were projected (as shown in Figure 6). Carbon storage decreases in both the natural development and cropland protection scenarios, while it increases in the ecological conservation scenario, as outlined in Table 7.

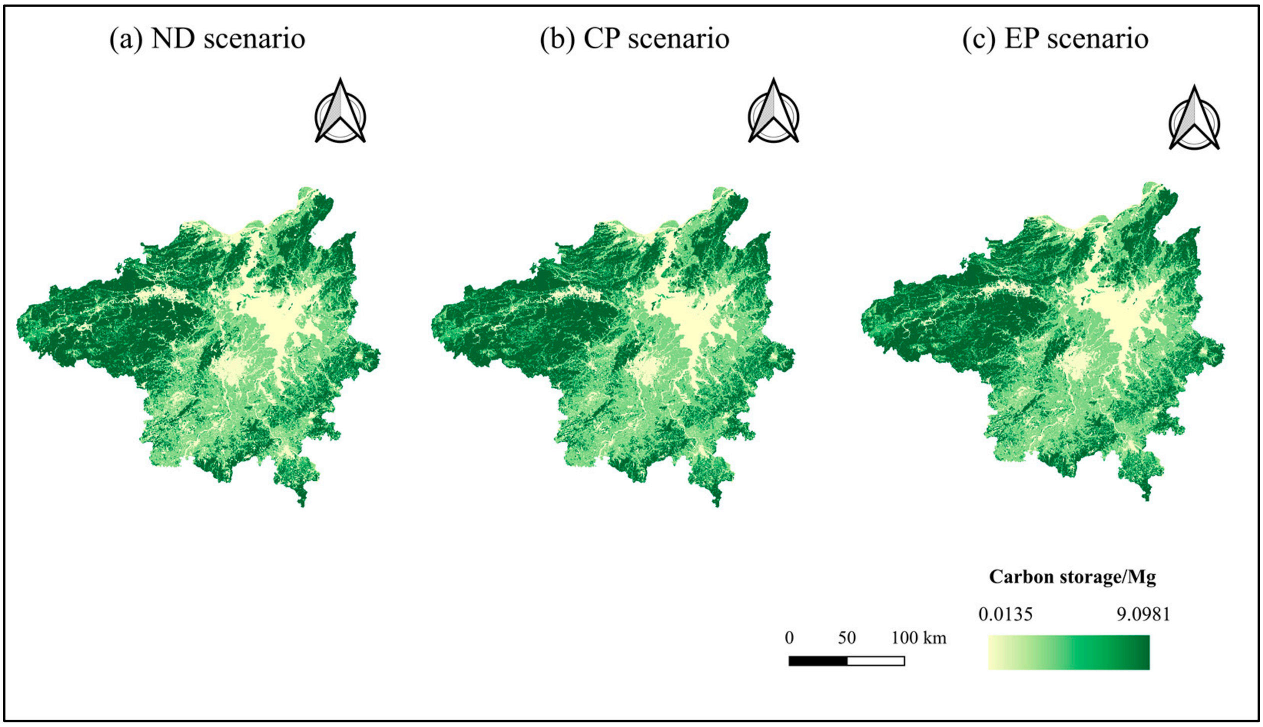


**Figure 6.** Simulation results of spatial distribution of carbon storage in 2040 under three scenarios.

**Table 7.** Prediction of land use structure and carbon storage of the study area in 2040.

| Scenario | Cropland | | Woodland | | Grassland | | Water Body | | Built-Up Land | | Unused Land | |
|---|---|---|---|---|---|---|---|---|---|---|---|---|
| | Area ($km^2$) | CS ($10^4$ t) | Area ($km^2$) | CS ($10^4$ t) | Area ($km^2$) | CS ($10^4$ t) | Area ($km^2$) | CS ($10^4$ t) | Area ($km^2$) | CS ($10^4$ t) | Area ($km^2$) | CS ($10^4$ t) |
| 2000 | 18,925.02 | 72.90 | 18,624.61 | 188.28 | 3102.30 | 19.36 | 5279.93 | 0.08 | 1027.54 | 0.19 | 164.27 | 0.04 |
| 2020 | 17,728.72 | 68.29 | 18,179.20 | 183.77 | 2718.48 | 16.97 | 5953.32 | 0.09 | 2480.28 | 0.47 | 62.73 | 0.02 |
| ND | 16,810.08 | 64.75 | 17,657.31 | 178.50 | 2485.21 | 15.51 | 6474.73 | 0.10 | 3653.73 | 0.69 | 41.67 | 0.01 |
| CP | 18,458.95 | 71.10 | 17,657.32 | 178.50 | 2485.22 | 15.51 | 5836.07 | 0.09 | 2648.12 | 0.50 | 37.05 | 0.01 |
| EP | 16,810.08 | 64.75 | 18,650.00 | 188.53 | 2550.38 | 15.92 | 6279.42 | 0.09 | 2795.79 | 0.53 | 37.05 | 0.01 |

CS indicates carbon storage.

In the ecological conservation scenario, carbon storage increases by $2.29 \times 10^5$ t. This scenario implements ecological conservation measures, which limit the reduction in ecological land and effectively control the continued conversion of cropland to built-up areas. Additionally, the rise in woodland areas also contributes to the overall increase in carbon storage. In the cropland protection scenario, carbon storage decreases by $3.90 \times 10^6$ t, primarily due to a decline in woodland area. Under the natural development scenario, carbon storage decreases by $1.00 \times 10^7$ t, which is more significant compared to that in the cropland protection scenario. This decrease is primarily caused by reductions in cropland, woodland, and water bodies, following the decreasing trend observed from 2000 to 2020. In conclusion, the natural development scenario exhibits the highest decrease. In contrast, the ecological conservation scenario demonstrates a substantial increase in carbon storage, while the cropland protection scenario effectively controls the decline in carbon storage.

Therefore, by 2040, it is recommended to implement ecological conservation measures based on cropland protection to effectively limit the expansion of built-up lands and to mitigate the reduction in carbon storage.

## 4. Discussion

### *4.1. Influence of Diverse Driving Factors on LUCC*

In this research endeavor, we conducted an assessment of the dynamic spatial allocation of LUCC within the Nanchang urban agglomeration spanning 2000 to 2020, encompassing three scenarios: natural development, cropland protection, and ecological conservation. The expansion of cropland, woodland, grassland, and built-up areas exhibited significant differences among the three scenarios. Figure 7 displays the hierarchical rankings of the significance of the causal factors influencing the expansion of the four categories of land use in the year 2020.

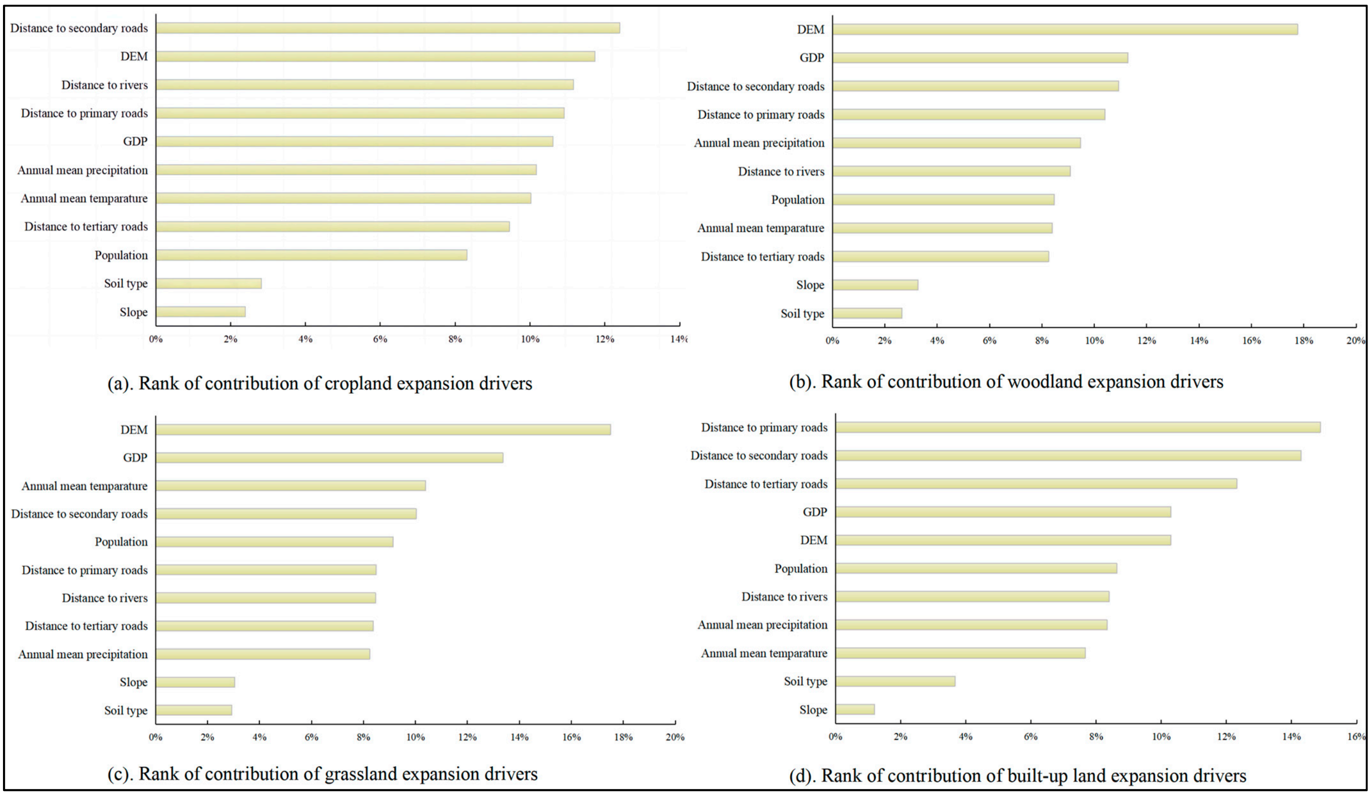


**Figure 7.** The rank of different drivers according to land use type.

Regarding cropland, we found that secondary roads exerted the most substantial influence on cropland growth. The development of the agricultural economy has necessitated the acceleration of agricultural product transportation from croplands to markets. For example, some research considers how agricultural supply chains and agricultural transportation have been impacted by the COVID-19 pandemic. [47]. The construction of secondary roads improves the transportation connectivity of rural areas surrounding the city, facilitating the transportation of agricultural products to markets within the urban region and increasing sales channels and opportunities. Additionally, the construction of secondary roads may enhance the infrastructure of rural areas, including water supply and drainage systems, thereby improving the land's usability and enabling the development of land that was previously unsuitable for agriculture. In promoting the construction of secondary roads, the government may also formulate corresponding agricultural development policies, which could include measures such as providing agricultural subsidies, technical support, and market orientation to encourage farmers to increase the area of cropland [48].

Therefore, it can be reasonably inferred that alterations in cropland extent are substantially impacted by the presence of secondary roads.

The primary factors driving the changes in woodland and grassland are altitude and GDP. On one hand, in the Nanchang urban agglomeration, higher-altitude regions typically have lower temperatures and higher rainfall, which are favorable for the growth of woodlands and grasslands. In the Vosges Mountains in north-eastern France, plants showed greater sensitivity to temperature at high elevation and to summer drought at low altitude and under dry conditions. [49]. Conversely, lower-altitude areas may face environmental issues such as water scarcity and land degradation, which can affect the quality and quantity of vegetation [50]. Furthermore, the Nanchang urban agglomeration is characterized by a higher level of economic development, indicating vigorous economic activities and an increased demand for land resources and development [51]. However, rapid economic development also brings about environmental challenges that need to be addressed [52,53]. Both the government and society have gradually recognized the importance of maintaining ecological balance and protecting natural resources, leading to an increasing emphasis on the conservation of forests, grasslands, and other ecosystems [54]. Relevant departments have implemented numerous ecological restoration and environmental governance measures to minimize the detrimental impacts of economic activities. In this context, although GDP growth is rapid, peoples' awareness of environmental protection has been heightened to maintain an ecological balance and achieve true sustainable development.

Roads are the primary factor influencing the expansion of built-up areas, with the three most significant contributing factors being primary roads, secondary roads, and tertiary roads. This indicates that built-up areas are more sensitive to road infrastructure. Primary roads, as the backbone of the urban road system, typically connect the city center with peripheral regions, effectively enhancing urban connectivity and radiance, attracting businesses, industries, and residents to expand outward. With the extension of primary roads, the land value in the surrounding areas gradually increases, further promoting the expansion of built-up areas. For example, some researchers have found that, in Beijing, changes in the expansion of the road core area are consistent with changes in the ecological risk level of the city center, mainly because of the spatial correlation between the two and the highway [55]. Secondary roads and tertiary roads mainly serve internal urban traffic, providing convenient travel environments. Secondary roads, as a supportive network for urban development, usually connect various primary roads and regional centers, contributing to the formation of a more intricate urban spatial pattern. Tertiary roads serve as community transportation networks, connecting different neighborhoods and residential areas, ensuring the daily travel needs of residents. The cooperation between secondary and tertiary roads advances the orderly development of urban built-up areas, implying that the expansion of the Nanchang urban agglomeration in 2040 will also be predominantly driven by road factors.

### 4.2. Impact of LUCC on Carbon Storage

LUCC is a significant driver of carbon storage fluctuations in terrestrial ecosystems. This is because different land cover types have varying levels of carbon storage capacity, and altering land use can lead to gains or losses in carbon storage. Drawing upon the land use transfer matrix for the Nanchang urban agglomeration from 2000 to 2020, and accounting for the disparities in carbon density among distinct land cover types, the calculation of carbon storage changes due to land use change revealed vegetation carbon storage in the Nanchang urban agglomeration decreased by $3.36 \times 10^6$ t, while soil carbon storage decreased by $7.89 \times 10^6$ t, resulting in a total carbon storage reduction of $11.25 \times 10^6$ t (Table 8).

**Table 8.** Changes in carbon storage caused by land use change.

| Land Use Type Conversion | | Area (km$^2$) | Changes in Vegetation Carbon Storage (×10$^6$ t) | Changes in Soil Carbon Storage (×10$^6$ t) | Total (×10$^6$ t) |
|---|---|---|---|---|---|
| Cropland | Wooldland | 842.379 | 4.419 | 0.852 | 5.271 |
| | Grassland | 346.527 | 0.133 | 0.695 | 0.828 |
| | Water body | 530.218 | −0.291 | −1.743 | −2.034 |
| | Built-up land | 1144.676 | −0.435 | −3.759 | −4.194 |
| | Unused land | 3.110 | −0.001 | −0.010 | −0.011 |
| Subtotal | | 2866.910 | 3.824 | −3.965 | −0.141 |
| Wooldland | Cropland | 909.391 | −4.771 | −0.919 | −5.690 |
| | Grassland | 720.920 | −3.506 | 0.718 | −2.788 |
| | Water body | 255.137 | −1.479 | −1.097 | −2.575 |
| | Built-up land | 190.862 | −1.074 | −0.820 | −1.894 |
| | Unused land | 0.805 | −0.005 | −0.003 | −0.008 |
| Subtotal | | 2077.115 | −10.833 | −2.121 | −12.955 |
| Grassland | Cropland | 384.664 | −0.147 | −0.772 | −0.919 |
| | Wooldland | 734.275 | 3.571 | −0.731 | 2.839 |
| | Water body | 193.863 | −0.181 | −1.027 | −1.207 |
| | Built-up land | 185.907 | −0.142 | −0.984 | −1.125 |
| | Unused land | 2.085 | −0.002 | −0.011 | −0.012 |
| Subtotal | | 1500.793 | 3.099 | −3.524 | −0.425 |
| Water body | Cropland | 258.840 | 0.142 | 0.851 | 0.993 |
| | Wooldland | 46.742 | 0.271 | 0.201 | 0.472 |
| | Grassland | 31.910 | 0.030 | 0.169 | 0.199 |
| | Built-up land | 54.471 | 0.009 | 0.000 | 0.009 |
| | Unused land | 12.852 | 0.001 | 0.002 | 0.003 |
| Subtotal | | 404.814 | 0.453 | 1.224 | 1.676 |
| Built-up land | Unused land | 101.111 | 0.038 | 0.332 | 0.370 |
| | Wooldland | 8.344 | 0.047 | 0.036 | 0.083 |
| | Grassland | 5.322 | 0.004 | 0.028 | 0.032 |
| | Water body | 11.990 | −0.002 | 0.000 | −0.002 |
| | Unused land | 0.141 | 0.000 | 0.000 | 0.000 |
| Subtotal | | 126.907 | 0.087 | 0.396 | 0.483 |
| Unused land | Unused land | 16.738 | 0.008 | 0.052 | 0.060 |
| | Wooldland | 0.482 | 0.003 | 0.002 | 0.005 |
| | Grassland | 12.347 | 0.011 | 0.063 | 0.074 |
| | Water body | 87.224 | −0.006 | −0.016 | −0.023 |
| | Built-up land | 3.743 | 0.000 | −0.001 | 0.000 |
| Subtotal | | 120.535 | 0.015 | 0.100 | 0.116 |
| Total | | 7097.073 | −3.355 | −7.891 | −11.245 |

The transformation of woodland and grassland into alternative land cover categories played a pivotal role in the noteworthy decline of carbon storage, resulting in a cumulative reduction of $1.34 \times 10^7$ t. Furthermore, carbon storage decreased as cropland and grassland were converted to built-up land, amounting to $4.19 \times 10^6$ t and $1.13 \times 10^6$ t, respectively, and accounting for 37.30% and 10.00% of the total carbon storage reduction. Conversely, the conversion of water body, built-up land, and unused land resulted in an augmentation of carbon storage by $1.68 \times 10^6$ t, $4.8 \times 10^5$ t, and $1.16 \times 10^5$ t, respectively. From 2020 to 2040, under natural development conditions, the same downward trend in carbon storage is observed for all types of features. Land use changes such as cropland-to-water body, cropland-to-built-up land, cropland-to-unused land, woodland-to-other land cover types, grassland-to-cropland, grassland-to-water body, grassland-to-built-up land, grassland-to-unused land, and unused land-to-water body all contributed to reductions in both vegetation and soil carbon storage. Conversely, transitions between other land cover types resulted in increases in both vegetation and soil carbon storage, facilitating carbon sequestration. From this, we find that the conversion of natural areas like woodland and grassland into built-up land can lead to significant carbon losses. To facilitate carbon storage in the region's woodland areas, we can identify suitable areas for reforestation and afforestation, especially in the study area, that were converted to non-vegetated land cover types, and we can plant native tree species that are well suited to the local climate and soil conditions, such as some subtropical fruit trees [56]. As for cropland, we can note some degree of cropland protection is effective in controlling carbon storage reductions. Poyang Lake Plain has a humid climate, a large area of arable land, and a high rate of cultivation. Thus, practical solutions such as promoting sustainable agricultural practices can reduce carbon emissions and enhance soil carbon sequestration. We also encourage no-till farming, cover cropping, and crop rotation to improve soil health and increase carbon storage in croplands. Some researchers have conducted crop rotation experiments in Denmark, and found that carbon storage accumulate rotationally during crop rotation [57]. Understanding the relationship between LUCC and carbon storage is crucial for effective land use planning and carbon management strategies. Policymakers and urban planners should consider the carbon implications of land use decisions.

### *4.3. Limitations and Future Work*

The amalgamation of PLUS and InVEST models effectively compensated for the limitations inherent in the individual models in this study, harnessing the quantitative and spatial simulation capabilities of the PLUS model in projecting forthcoming land use transformations, while capitalizing on the InVEST model's strengths in forecasting carbon storage dynamics. An inherent limitation of this investigation lies in the fact that there exists a disparity between the three categories of developmental models employed and the actual unfolding of development scenarios. This discrepancy restricts the ability to encompass the entirety of potential future development trajectories. Integrating policy considerations to establish a more pragmatic estimate of future land use demand and reducing the disparity between projected development scenarios and actual development models will undoubtedly constitute central emphases in the realm of research concerning the simulation of prospective land use transformations.

Carbon density varies over time and is influenced by factors like precipitation, temperature, and soil organic carbon sensitivity. Additionally, the study area's significant elevation difference (~2000 m) indirectly affects carbon storage. In future work, this should be addressed at a fine spatial and temporal scale to capture variations within the study area. In some of the studies that have been carried out, for example, scholars have begun to assess the dynamic carbon neutral potential of urban neighborhoods as basic units of cities [58], which could have implications for future work. At the same time, there is a need for field sampling and regular updating of carbon pools, relying on laboratory analyses and existing data, and the use of statistical analyses, such as regression models, to assess the effects of precipitation, temperature, and soil organic carbon sensitivity [59].

In the selection of multi-scenario setting methods, the Markov chain method based on quantitative constraints for multiple scenarios is the most mainstream practice, but the parameter settings are also relatively more subjective, and in future research, attempts at linear programming methods can better enhance regional carbon storage.

In addition, the scope of the study can be expanded to analyze the carbon storage changes among different urban agglomerations, and the relationship between land drivers and carbon storage can be more comprehensively analyzed.

## 5. Conclusions

The PLUS and InVEST models were combined to validate the PLUS model using historical land use data from the Nanchang urban agglomeration in 2000 and 2020. This was conducted to simulate the LUCC in the Nanchang urban agglomeration in 2040 under different policy-driven scenarios: natural development (ND), cropland protection (CP), and ecological protection (EP). Additionally, the InVEST model was employed to conduct an analysis of carbon storage and understand how land use patterns might impact carbon storage in the Nanchang urban agglomeration. The potential impact of land use patterns on carbon storage in the Nanchang urban agglomeration were clarified. The following conclusions were reached:

(1) From 2000 to 2020, cropland became a significant source of rapid expansion of built-up areas in the Nanchang urban agglomeration, with a conversion area of 2866.91 $km^2$. Under the CP and EP scenarios, compared to the ND scenario, cropland and forestland areas increased by 9.30% and 5.46%, respectively.

(2) Carbon storage in the Nanchang urban agglomeration amounted to $2.81 \times 10^8$ t in 2000 and $2.70 \times 10^8$ t in 2020. Regions characterized by diminished carbon storage are notably conspicuous within the central zone of the urban agglomeration, concentrated in Nanchang City. Cropland encroachment in the region is an important cause of declining carbon storage.

(3) In the context of the ND scenario, it is projected that carbon storage within the Nanchang urban agglomeration in the year 2040 will experience a reduction of $1.00 \times 10^7$ t in comparison to the levels observed in 2020. Under the EP scenario, carbon storage is estimated to increase by $2.29 \times 10^5$ t by 2040, indicating that implementing certain ecological protection measures can effectively reduce the declining trend of carbon storage within the study area. Additionally, the conservation of woodlands around urban agglomerations contributes to the regional carbon sink potential.

**Author Contributions:** Y.F. (Yuheng Fu); writing—original draft, data curation, formal analysis, investigation, methodology, software, conceptualization, and visualization. M.H.; writing—original draft, investigation, methodology, conceptualization, and funding acquisition. D.G.; writing—review and editing. H.L.; writing—review and editing. Y.F. (Yewen Fan); writing—review and editing. W.D.; writing—review and editing. All authors have read and agreed to the published version of the manuscript.

**Funding:** This work was supported by the National Nature Science Foundation of China (NSFC) program (No. 42201438), the Youth Program of Major Discipline Academic and Technical Leaders Training Program of Jiangxi Talents Supporting Project (No. 20232BCJ23086), Open Research Fund Program of LIESMARS (Grant No. 22I01), Open Fund of National Engineering Research Center for Geographic Information System, China University of Geosciences, Wuhan 430074, China (Grant No. 2021KFJJ07), the Opening Fund of Key Laboratory of Poyang Lake Wetland and Watershed Research (Jiangxi Normal University), Ministry of Education (No. PK2022001) and the talent startup fund of Jiangxi Normal University.

**Data Availability Statement:** The data presented in this study are cited within the article.

**Acknowledgments:** We appreciate the constructive suggestions and comments from the editor and anonymous reviewers.

**Conflicts of Interest:** The authors declare no conflict of interest.

## References

1. Riahi, K.; van Vuuren, D.P.; Kriegler, E.; Edmonds, J.; O'Neill, B.C.; Fujimori, S.; Bauer, N.; Calvin, K.; Dellink, R.; Fricko, O.; et al. The Shared Socioeconomic Pathways and their energy, land use, and greenhouse gas emissions implications: An overview. *Glob. Environ. Chang. Hum. Policy Dimens.* **2017**, *42*, 153–168. [CrossRef]
2. Destek, M.A.; Sarkodie, S.A. Investigation of environmental Kuznets curve for ecological footprint: The role of energy and financial development. *Sci. Total Environ.* **2019**, *650*, 2483–2489. [CrossRef] [PubMed]
3. Chen, X.; Li, N.; Kong, Z.; Ong, W.-J.; Zhao, X. Photocatalytic fixation of nitrogen to ammonia: State-of-the-art advancements and future prospects. *Mater. Horiz.* **2018**, *5*, 9–27. [CrossRef]

4. Sala, O.E.; Chapin, F.S., 3rd; Armesto, J.J.; Berlow, E.; Bloomfield, J.; Dirzo, R.; Huber-Sanwald, E.; Huenneke, L.F.; Jackson, R.B.; Kinzig, A.; et al. Global biodiversity scenarios for the year 2100. *Science* **2000**, *287*, 1770–1774. [CrossRef] [PubMed]
5. Buonincontri, M.P.; Bosso, L.; Smeraldo, S.; Chiusano, M.L.; Pasta, S.; Di Pasquale, G. Shedding light on the effects of climate and anthropogenic pressures on the disappearance of *Fagus sylvatica* in the Italian lowlands: Evidence from archaeo-anthracology and spatial analyses. *Sci. Total Environ.* **2023**, *877*, 162893. [CrossRef] [PubMed]
6. Dogu, O.; Pelucchi, M.; Van de Vijver, R.; Van Steenberge, P.H.M.; D'Hooge, D.R.; Cuoci, A.; Mehl, M.; Frassoldati, A.; Faravelli, T.; Van Geem, K.M. The chemistry of chemical recycling of solid plastic waste via pyrolysis and gasification: State-of-the-art, challenges, and future directions. *Prog. Energy Combust. Sci.* **2021**, *84*, 100901. [CrossRef]
7. Shen, M.; Huang, W.; Chen, M.; Song, B.; Zeng, G.; Zhang, Y. (Micro)plastic crisis: Un-ignorable contribution to global greenhouse gas emissions and climate change. *J. Clean. Prod.* **2020**, *254*, 120138. [CrossRef]
8. Shih, C.F.; Zhang, T.; Li, J.; Bai, C. Powering the Future with Liquid Sunshine. *Joule* **2018**, *2*, 1925–1949. [CrossRef]
9. Liu, Z.; Deng, Z.; He, G.; Wang, H.; Zhang, X.; Lin, J.; Qi, Y.; Liang, X. Challenges and opportunities for carbon neutrality in China. *Nat. Rev. Earth Environ.* **2022**, *3*, 141–155. [CrossRef]
10. Zhao, X.; Ma, X.; Chen, B.; Shang, Y.; Song, M. Challenges toward carbon neutrality in China: Strategies and countermeasures. *Resour. Conserv. Recycl.* **2022**, *176*, 105959. [CrossRef]
11. Yang, Y.; Shi, Y.; Sun, W.; Chang, J.; Zhu, J.; Chen, L.; Wang, X.; Guo, Y.; Zhang, H.; Yu, L.; et al. Terrestrial carbon sinks in China and around the world and their contribution to carbon neutrality. *Sci. China Life Sci.* **2022**, *65*, 861–895. [CrossRef]
12. Poorter, L.; van der Sande, M.T.; Thompson, J.; Arets, E.J.M.M.; Alarcon, A.; Alvarez-Sanchez, J.; Ascarrunz, N.; Balvanera, P.; Barajas-Guzman, G.; Boit, A.; et al. Diversity enhances carbon storage in tropical forests. *Glob. Ecol. Biogeogr.* **2015**, *24*, 1314–1328. [CrossRef]
13. Lehmann, J.; Cowie, A.; Masiello, C.A.; Kammann, C.; Woolf, D.; Amonette, J.E.; Cayuela, M.L.; Camps-Arbestain, M.; Whitman, T. Biochar in climate change mitigation. *Nat. Geosci.* **2021**, *14*, 883–892. [CrossRef]
14. Xia, L.; Lam, S.K.; Wolf, B.; Kiese, R.; Chen, D.; Butterbach-Bahl, K. Trade-offs between soil carbon sequestration and reactive nitrogen losses under straw return in global agroecosystems. *Glob. Chang. Biol.* **2018**, *24*, 5919–5932. [CrossRef] [PubMed]
15. Chai, J.; Wu, H.; Hao, Y. Planned economic growth and controlled energy demand: How do regional growth targets affect energy consumption in China? *Technol. Forecast. Soc. Chang.* **2022**, *185*, 122068. [CrossRef]
16. Li, Y.; Li, Y.; Chang, S.X.; Yang, Y.; Fu, S.; Jiang, P.; Luo, Y.; Yang, M.; Chen, Z.; Hu, S.; et al. Biochar reduces soil heterotrophic respiration in a subtropical plantation through increasing soil organic carbon recalcitrancy and decreasing carbon degrading microbial activity. *Soil Biol. Biochem.* **2018**, *122*, 173–185. [CrossRef]
17. Lyu, R.; Zhang, J.; Xu, M.; Li, J. Impacts of urbanization on ecosystem services and their temporal relations: A case study in Northern Ningxia, China. *Land Use Policy* **2018**, *77*, 163–173. [CrossRef]
18. Holmes, K.W.; Wherrett, A.; Keating, A.; Murphy, D.V. Meeting bulk density sampling requirements efficiently to estimate soil carbon stocks. *Soil Res.* **2011**, *49*, 680–695. [CrossRef]
19. Angelopoulou, T.; Tziolas, N.; Balafoutis, A.; Zalidis, G.; Bochtis, D. Remote Sensing Techniques for Soil Organic Carbon Estimation: A Review. *Remote Sens.* **2019**, *11*, 676. [CrossRef]
20. Zhang, Y.; Hui, J.; Qin, Q.; Sun, Y.; Zhang, T.; Sun, H.; Li, M. Transfer-learning-based approach for leaf chlorophyll content estimation of winter wheat from hyperspectral data. *Remote Sens. Environ.* **2021**, *267*, 112724. [CrossRef]
21. Olofsson, P.; Foody, G.M.; Stehman, S.V.; Woodcock, C.E. Making better use of accuracy data in land change studies: Estimating accuracy and area and quantifying uncertainty using stratified estimation. *Remote Sens. Environ.* **2013**, *129*, 122–131. [CrossRef]
22. Searchinger, T.D.; Wirsenius, S.; Beringer, T.; Dumas, P. Assessing the efficiency of changes in land use for mitigating climate change. *Nature* **2018**, *564*, 249–253. [CrossRef]
23. Sun, L.-L.; Cui, H.-J.; Ge, Q.-S. Will China achieve its 2060 carbon neutral commitment from the provincial perspective? *Adv. Clim. Chang. Res.* **2022**, *13*, 169–178. [CrossRef]
24. Regnier, P.; Resplandy, L.; Najjar, R.G.; Ciais, P. The land-to-ocean loops of the global carbon cycle. *Nature* **2022**, *603*, 401–410. [CrossRef] [PubMed]
25. Fang, Z.; Ding, T.; Chen, J.; Xue, S.; Zhou, Q.; Wang, Y.; Wang, Y.; Huang, Z.; Yang, S. Impacts of land use/land cover changes on ecosystem services in ecologically fragile regions. *Sci. Total Environ.* **2022**, *831*, 154967. [CrossRef]
26. Leh, M.D.K.; Matlock, M.D.; Cummings, E.C.; Nalley, L.L. Quantifying and mapping multiple ecosystem services change in West Africa. *Agric. Ecosyst. Environ.* **2013**, *165*, 6–18. [CrossRef]
27. He, C.; Zhang, D.; Huang, Q.; Zhao, Y. Assessing the potential impacts of urban expansion on regional carbon storage by linking the LUSD-urban and InVEST models. *Environ. Model. Softw.* **2016**, *75*, 44–58. [CrossRef]
28. Babbar, D.; Areendran, G.; Sahana, M.; Sarma, K.; Raj, K.; Sivadas, A. Assessment and prediction of carbon sequestration using Markov chain and InVEST model in Sariska Tiger Reserve, India. *J. Clean. Prod.* **2021**, *278*, 123333. [CrossRef]
29. Wang, Z.; Li, X.; Mao, Y.; Li, L.; Wang, X.; Lin, Q. Dynamic simulation of land use change and assessment of carbon storage based on climate change scenarios at the city level: A case study of Bortala, China. *Ecol. Indic.* **2022**, *134*, 108499. [CrossRef]
30. Zhu, G.; Qiu, D.; Zhang, Z.; Sang, L.; Liu, Y.; Wang, L.; Zhao, K.; Ma, H.; Xu, Y.; Wan, Q. Land-use changes lead to a decrease in carbon storage in arid region, China. *Ecol. Indic.* **2021**, *127*, 107770. [CrossRef]
31. Xia, C.; Zhang, J.; Zhao, J.; Xue, F.; Li, Q.; Fang, K.; Shao, Z.; Li, S.; Zhou, J. Exploring potential of urban land-use management on carbon emissions—A case of Hangzhou, China. *Ecol. Indic.* **2023**, *146*, 109902. [CrossRef]

32. Chen, Z.; Huang, M.; Zhu, D.; Altan, O. Integrating Remote Sensing and a Markov-FLUS Model to Simulate Future Land Use Changes in Hokkaido, Japan. *Remote Sens.* **2021**, *13*, 2621. [CrossRef]
33. Peng, J.; Hu, X.; Wang, X.; Meersmans, J.; Liu, Y.; Qiu, S. Simulating the impact of Grain-for-Green Programme on ecosystem services trade-offs in Northwestern Yunnan, China. *Ecosyst. Serv.* **2019**, *39*, 100998. [CrossRef]
34. Pala, L.P.R.; Wang, Q.; Kolb, G.; Liessel, V. Steam gasification of biomass with subsequent syngas adjustment using shift reaction for syngas production: An Aspen Plus model. *Renew. Energy* **2017**, *101*, 484–492. [CrossRef]
35. Zhang, S.; Zhong, Q.; Cheng, D.; Xu, C.; Chang, Y.; Lin, Y.; Li, B. Landscape ecological risk projection based on the PLUS model under the localized shared socioeconomic pathways in the Fujian Delta region. *Ecol. Indic.* **2022**, *136*, 108642. [CrossRef]
36. Lawler, J.J.; Lewis, D.J.; Nelson, E.; Plantinga, A.J.; Polasky, S.; Withey, J.C.; Helmers, D.P.; Martinuzzi, S.; Pennington, D.; Radeloff, V.C. Projected land-use change impacts on ecosystem services in the United States. *Proc. Natl. Acad. Sci. USA* **2014**, *111*, 7492–7497. [CrossRef]
37. Zhang, C.-y.; Zhao, L.; Zhang, H.; Chen, M.-n.; Fang, R.-y.; Yao, Y.; Zhang, Q.-p.; Wang, Q. Spatial-temporal characteristics of carbon emissions from land use change in Yellow River Delta region, China. *Ecol. Indic.* **2022**, *136*, 108623. [CrossRef]
38. Tong, X.; Brandt, M.; Yue, Y.; Ciais, P.; Jepsen, M.R.; Penuelas, J.; Wigneron, J.-P.; Xiao, X.; Song, X.-P.; Horion, S.; et al. Forest management in southern China generates short term extensive carbon sequestration. *Nat. Commun.* **2020**, *11*, 129. [CrossRef]
39. Jia, M.M.; Wang, Z.M.; Mao, D.H.; Ren, C.Y.; Song, K.S.; Zhao, C.P.; Wang, C.; Xiao, X.M.; Wang, Y.Q. Mapping global distribution of mangrove forests at 10-m resolution. *Sci. Bull.* **2023**, *68*, 1306–1316. [CrossRef]
40. Li, J.; Wen, Y.; Li, X.; Li, Y.; Yang, X.; Lin, Z.; Song, Z.; Cooper, J.M.; Zhao, B. Soil labile organic carbon fractions and soil organic carbon stocks as affected by long-term organic and mineral fertilization regimes in the North China Plain. *Soil Tillage Res.* **2018**, *175*, 281–290. [CrossRef]
41. Piao, S.; He, Y.; Wang, X.; Chen, F. Estimation of China's terrestrial ecosystem carbon sink: Methods, progress and prospects. *Sci. China Earth Sci.* **2022**, *65*, 641–651. [CrossRef]
42. Liu, L.; Chen, C.; Zhao, Y.; Zhao, E. China's carbon-emissions trading: Overview, challenges and future. *Renew. Sustain. Energy Rev.* **2015**, *49*, 254–266. [CrossRef]
43. Ma, L.; Xiang, L.G.; Wang, C.; Chen, N.C.; Wang, W. Spatiotemporal evolution of urban carbon balance and its response to new-type urbanization: A case of the middle reaches of the Yangtze River Urban Agglomerations, China. *J. Clean. Prod.* **2022**, *380*, 135122. [CrossRef]
44. Huang, S.Z.; Gan, Y.; Zhang, X.; Chen, N.C.; Wang, C.; Gu, X.H.; Ma, J.J.; Niyogi, D. Urbanization Amplified Asymmetrical Changes of Rainfall and Exacerbated Drought: Analysis Over Five Urban Agglomerations in the Yangtze River Basin, China. *Earths Future* **2023**, *11*, e2022EF003117. [CrossRef]
45. Wang, L.; Yi, C.; Xu, X.; Schuett, B.; Liu, K.; Zhou, L. Soil properties in two soil profiles from terraces of the Nam Co Lake in Tibet, China. *J. Mt. Sci.* **2009**, *6*, 354–361. [CrossRef]
46. Niu, D.; Wang, S.; Ouyang, Z. Comparisons of carbon storages in Cunninghamia lanceolata and *Michelia macclurei* plantations during a 22-year period in southern China. *J. Environ. Sci.* **2009**, *21*, 801–805. [CrossRef]
47. Gray, R.S. Agriculture, transportation, and the COVID-19 crisis. *Can. J. Agric. Econ. Rev. Can. D Agroecon.* **2020**, *68*, 239–243. [CrossRef]
48. Piquer-Rodriguez, M.; Butsic, V.; Gaertner, P.; Macchi, L.; Baumann, M.; Pizarro, G.G.; Volante, J.N.; Gasparri, I.N.; Kuemmerle, T. Drivers of agricultural land-use change in the Argentine Pampas and Chaco regions. *Appl. Geogr.* **2018**, *91*, 111–122. [CrossRef]
49. Lebourgeois, F.; Gomez, N.; Pinto, P.; Merian, P. Mixed stands reduce Abies alba tree-ring sensitivity to summer drought in the Vosges mountains, western Europe. *For. Ecol. Manag.* **2013**, *303*, 61–71. [CrossRef]
50. Messerli, B.; Viviroli, D.; Weingartner, R. Mountains of the world: Vulnerable Water Towers for the 21(st) century. *Ambio* **2004**, *33*, 29–34. [CrossRef]
51. Popp, A.; Calvin, K.; Fujimori, S.; Havlik, P.; Humpenoeder, F.; Stehfest, E.; Bodirsky, B.L.; Dietrich, J.P.; Doelmann, J.C.; Gusti, M.; et al. Land-use futures in the shared socio-economic pathways. *Glob. Environ. Chang. Hum. Policy Dimens.* **2017**, *42*, 331–345. [CrossRef]
52. Bandyopadhyay, A.; Heer, B. Additive manufacturing of multi-material structures. *Mater. Sci. Eng. R Rep.* **2018**, *129*, 1–16. [CrossRef]
53. Reis, R.S.; Salvo, D.; Ogilvie, D.; Lambert, E.V.; Goenka, S.; Brownson, R.C.; Lancet Phys Act Series, E. Scaling up physical activity interventions worldwide: Stepping up to larger and smarter approaches to get people moving. *Lancet* **2016**, *388*, 1337–1348. [CrossRef] [PubMed]
54. Sklar, F.H.; Chimney, M.J.; Newman, S.; McCormick, P.; Gawlik, D.; Miao, S.L.; McVoy, C.; Said, W.; Newman, J.; Coronado, C.; et al. The ecological-societal underpinnings of Everglades restoration. *Front. Ecol. Environ.* **2005**, *3*, 161–169. [CrossRef]
55. Mo, W.; Wang, Y.; Zhang, Y.; Zhuang, D. Impacts of road network expansion on landscape ecological risk in a megacity, China: A case study of Beijing. *Sci. Total Environ.* **2017**, *574*, 1000–1011. [CrossRef] [PubMed]
56. Lazaro-Lobo, A.; Ruiz-Benito, P.; Cruz-Alonso, V.; Castro-Diez, P. Quantifying carbon storage and sequestration by native and non-native forests under contrasting climate types. *Glob. Chang. Biol.* **2023**, *29*, 4530–4542. [CrossRef]
57. Knudsen, M.T.; Meyer-Aurich, A.; Olesen, J.E.; Chirinda, N.; Hermansen, J.E. Carbon footprints of crops from organic and conventional arable crop rotations—Using a life cycle assessment approach. *J. Clean. Prod.* **2014**, *64*, 609–618. [CrossRef]

58. Ye, H.; Li, Y.; Shi, D.; Meng, D.; Zhang, N.; Zhao, H. Evaluating the potential of achieving carbon neutrality at the neighborhood scale in urban areas. *Sustain. Cities Soc.* **2023**, *97*, 104764. [CrossRef]
59. Elliot, T.; Bertrand, A.; Almenar, J.B.; Petucco, C.; Proenca, V.; Rugani, B. Spatial optimisation of urban ecosystem services through integrated participatory and multi-objective integer linear programming. *Ecol. Model.* **2019**, *409*, 108774. [CrossRef]